International Journal of Computer Applications (0975 - 8887)
Volume 186 - No.45, October 2024

An Efficient Restoration Method for the Faint Dot Matrix Images

Ao Zhu
Beijing Institute of Graphic Communication
No.1, Section 2, Xinghua Street Daxing District
Beijing 102600, China

Peng Cao
Beijing Institute of Graphic Communication
No.1, Section 2, Xinghua Street Daxing District
Beijing 102600, China

ABSTRACT

This study introduces an innovative image processing approach that integrates U-Net with Generative Adversarial Networks (GANs) for the efficient restoration and decoding of printed faint dot matrix images, aiming to enhance the application of anti-counterfeiting technologies. By merging the encoding and decoding capabilities of U-Net with the adversarial generation mechanisms of GANs, this method accurately extracts faint anti-counterfeiting features within complex noisy and blurring backgrounds, significantly improving image clarity and readability. Central to this approach are the incorporation of a Gradient-Sensitive Activation (GSA) function and a roughening term in the loss function, which are specifically optimized for high-gradient areas and detail capture. Moreover, the system dynamically adjusts network weights based on decoding rate feedback to optimize the image restoration process. Experimental results demonstrate that this method has image clarity, readability, and decoding accuracy for the faint dot matrix images. This technology has broad application prospects in industries with high security demands, such as e-commerce and product packaging.

General Terms

Image Processing, Deep Learning

Keywords

GANs; U-Net; Anti-counterfeiting Technology; Gradient-sensitive Activation (GSA); Dot Matrix Image; High-gradient Image Enhancement; Security Features in Printing

1. INTRODUCTION

In today's era of rapid digitalization and information technology advancement, image processing technology has become an indispensable part of modern communication, anti-counterfeiting security [1], and data management. Particularly in the field of anti-counterfeiting technology [2, 3, 4], as counterfeit and inferior products proliferate, the effective identification and verification of authenticity have emerged as urgent issues to address. Traditional anti-counterfeiting technologies, such as watermarks [5] and holograms [6, 7], provide a degree of security but often fall short in the face of advanced replication techniques. Thus, developing a more efficient and difficult-to-crack new anti-counterfeiting technology is imperative.

In recent years, the advent of deep learning has propelled technologies like Generative Adversarial Networks (GANs) [8] and Variational Autoencoders (VAEs) [9] into the limelight within the realms of image generation, editing, and enhancement. These models excel by producing high-quality, detail-rich images, crucial for the complex tasks of image restoration and enhancement. Particularly in the anti-counterfeiting domain [1, 10, 11], these technologies offer a novel approach—enhancing image security features through complex generative models, making forgery increasingly challenging. In [10], authors combined the capacities of deep learning and the Generative Adversarial Network (GAN) [8] to deal with anti-counterfeit handwritten signature. In [11], the proposed detection method based on deep learning can prevent personal monetary damages caused by counterfeit bills. In [1], Teymournezhad et al. developed a novel method to identify counterfeit banknotes using the security components based on both image processing and GoogLeNet deep learning network.

This research builds upon previous work, focusing especially on a technique known as the restoration and decoding of printed faint dot matrix images. Leveraging deep learning's U-Net [12] and Generative Adversarial Networks (GANs) [8], this technique not only enhances the visual quality of images but more importantly, improves the decoding accuracy of the invisible dot matrix within them. A dot matrix image is a type of image that is created using a grid of dots, where each dot represents a pixel in the image. The image is made up of a series of dots that are either turned on or off to create the desired image. Dot matrix images are commonly used in older printers and displays, where the image is created by printing or displaying a series of dots in a grid pattern. The printed image is composed of halftone dots and these dots have regular arrangement [13]. The digital halftoning is a technique for converting continuous-tone images into binary images [14, 15]. For recovering hidden binary data, the author in [16] proposed a decoding method to estimate embedded data from clustered halftone dots using learned dictionary. Printed quantum dots are usually single halftone outlets that are very small indivisible printing imaging units of recording information [17]. Printed quantum dots record information and load it into complex image to realize printing information anti-counterfeiting [18]. The quantum dots-based middle-far-infrared detection and imaging method is proposed by Chen

et al. [19]. The ethanol vapor sensor based on a microfiber with a quantum-dot gel coating is also proposed and demonstrated in [20]. Esfahani et al. [21] developed the superlens with high resolution via quantum dot nano-particles. Based on error controlling, Li et al. in [22] presented an approach to the vectorization of dot matrix image. In [23], Xu et al. presented the indirected method to construct clustered dot dithering matrix. Cheng Y. proposed a scanning method for dotted data matrix in [24]. The dot matrix text recognition can be used for industrial carton classification [25]. Image recognition technique for dot-matrix character on piston surface is developed on hopfield neural network method in [26]. The recognition method of dot-matrix character-degraded has been proposed using the affine registration [27]. Dot matrix images, a common anti-counterfeiting technique, typically embed information in minute dot patterns that are difficult to discern or read by the naked eye or machines without special processing. The customized 2D barcode sensing for anti-counterfeiting can be applied in the Internet of Things [28]. Wang et al. in [29] designed a texture-hidden QR coding method to prevent the illegal copying of a QR code. For dot matrix images, image degradation will not only affect the deterioration of its visual effects but also seriously affect the decoding and reading of image information. The methods of restoring image details are mainly divided into two categories: traditional methods and deep learning methods. Traditional image restoration uses filtering methods to repair the missing or blurred parts of the image. The Wiener filtering is the important filtering method that can be used to restore the dot matrix image effectively [30, 31, 32]. Deep learning methods use multi-layer networks [33, 34, 35] to learn models from a large amount of input sample data for recovering images. In this paper, we apply deep learning models to restore damaged dot matrix images and accurately decode the embedded information.

In this study, U-Net based architecture [12] is employed as the generator and a convolutional PatchGAN classifier [36] is used as the discriminator to form the U-Net based GAN model. In the proposed model, the learned high-level features assist in better restoring and interpreting the invisible dot matrices. Moreover, an activation function called Gradient-Sensitive Activation (GSA) is introduced to enhance the model's sensitivity to high-gradient changes in the image, thereby preserving more detail during image restoration. To further improve model performance and adaptability, a roughening term is incorporating in the loss function. This term enables the model to focus more on specific areas of the image (such as high-gradient or low-contrast areas), effectively enhancing the recognition and restoration capabilities for subtle anti-counterfeiting features.

Additionally, this research adopts an adaptive network weight updating mechanism, which optimizes image processing workflows and significantly enhances the stability and reliability of the decoding process by dynamically monitoring the dot matrix's decoding rate. Extensive experimental validations demonstrate that the proposed model performs excellently in the restoration and decoding tasks of printed faint dot matrix images. Results indicate that the proposed approach achieves better fidelity and decoding accuracy and significantly faster processing speeds. Furthermore, the potential applications of this technology are vast, not only in high-security anti-counterfeiting areas such as currency and document protection but also extending to e-commerce, packaging printing, and product traceability.

This paper not only demonstrates the potential application of deep learning in image anti-counterfeiting technology but also provides a new perspective and methodology for future research in image processing technology. As these technologies continue to evolve and improve, deep learning is expected to play an increasingly significant role in protecting intellectual property, ensuring data security, and combating illegal reproductions.

2. RELATED WORK

2.1 U-Net Architecture

The U-Net architecture is composed of a contracting path (encoder) and an expansive path (decoder). The encoder consists of convolutional layers that progressively downsample the input image, capturing context and high-level features:

$$\mathbf{z} = E(\mathbf{x}) = \sigma\left(W_{E,n} * \sigma\left(\cdots \sigma\left(W_{E,2} * \sigma\left(W_{E,1} * \mathbf{x} + b_{E,1}\right) + b_{E,2}\right)\cdots\right) + b_{E,n}\right) \quad (1)$$

where $\mathbf{x}$ is the input image, $\mathbf{z}$ is the latent representation, $W_{E,i}$ and $b_{E,i}$ are the weights and biases of the encoder layers, σ is the activation function (typically ReLU), and $*$ denotes the convolution operation.

The decoder then up-samples this compressed representation to reconstruct the image, often using transposed convolutions:

$$\hat{\mathbf{x}} = D(\mathbf{z}) = \sigma\left(W_{D,1} *^T \sigma\left(W_{D,2} *^T \sigma\left(\cdots \sigma\left(W_{D,n} *^T \mathbf{z} + b_{D,n}\right)\cdots\right) + b_{D,2}\right) + b_{D,1}\right) \quad (2)$$

where $W_{D,i}$ and $b_{D,i}$ are the weights and biases of the decoder layers, and $*^T$ denotes the transposed convolution.
U-Net is particularly effective in preserving gradient information due to its skip connections, which directly transfer low-level features from the encoder to the decoder, maintaining high-resolution details. This feature is crucial for high-gradient areas where fine details are essential.

2.2 GANs in Image Restoration

GANs consist of a generator G and a discriminator D that are trained adversarially. The generator attempts to produce images that are indistinguishable from real images, while the discriminator aims to differentiate between real and generated images. The loss functions for the GAN components are defined as:

$$\min_G \max_D \mathbb{E}_{\mathbf{x}\sim p_{\text{data}}(\mathbf{x})}\left[\log D(\mathbf{x})\right] + \mathbb{E}_{\mathbf{z}\sim p_{\mathbf{z}}(\mathbf{z})}\left[\log\left(1 - D(G(\mathbf{z}))\right)\right] \quad (3)$$

where $p_{\text{data}}(\mathbf{x})$ is the distribution of real images and $p_{\mathbf{z}}(\mathbf{z})$ is the distribution of the latent space.

GANs [8] are particularly effective in enhancing the realism of high-gradient areas. The discriminator's role in enforcing high-frequency details ensures that the generator produces sharper and more realistic edges, which is critical for the accurate restoration of gradient-sensitive images.

GANs have been extensively studied since the publication in 2014. Their integrations with U-Net has greatly promoted the development of style transfer and image-to-image translation. In recent years, the U-Net based Generative Adversarial Network models [37, 38] are proposed for image generation tasks. In the U-Net based Generative Adversarial Network models, GAN models usually depend on convolution operations for feature extraction. So U-Net GANs [37, 38] can learn the differences in both global and local features to generate images that are realistic both globally and locally. In this paper, the proposed method is different from these U-Net based Generative Adversarial Network models, U-Net is used as the generator, and for the discriminator a convolutional

PatchGAN classifier [36] is used to penalize the information hides in the image patches.

3. METHODS

In this section, the detailed methodology is presented to develop our innovative image processing approach, which integrates U-Net with Generative Adversarial Networks (GANs) for the restoration and decoding of printed faint dot matrix images. This approach aims to enhance anti-counterfeiting technologies by improving image clarity and readability through several key innovations, including the incorporation of a gradient-sensitive activation (GSA) function, a roughening term in the loss function, a decoding module with feedback mechanism, and a dynamic weight adjustment mechanism.

3.1 The Overall Architecture of the Proposed U-Net GAN

The overall architecture of the U-Net based generative adversarial network is divided into two parts that are the U-Net based generative adversarial network and the U-Net based generative adversarial network. The part 1 corresponding to the U-Net based generative adversarial network is shown in Figure 1.

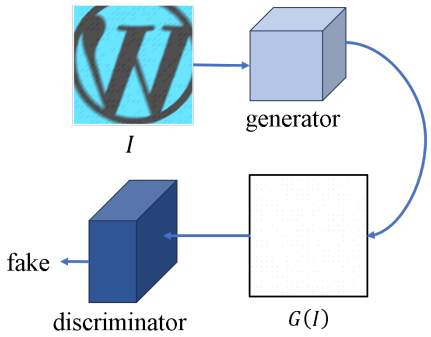

Fig. 1: The U-Net based generative adversarial network.

It is the path that learns a mapping from the noisy and blurring image I containing faint dot matrix information to the real dot matrix image J. the U-Net [12] is ued as the generator, which is trained to produce $G(I)$ that cannot be distinguished from the real dot matrix image J by the discriminator that is the PatchGAN classifier [36]. The part 2 corresponding to the U-Net based generative adversarial network is shown in Figure 2.

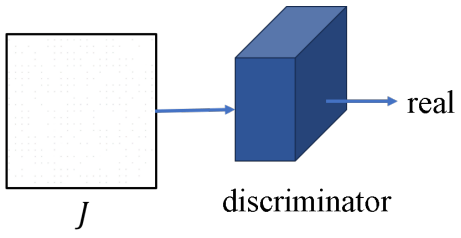

Fig. 2: The U-Net based generative adversarial network.

It is a path that maps from the real dot matrix image J to detect the real output by the discriminator.

3.1.1 The U-Net Based Generator. For the previous encoder-decoder network [39], the input is passed through a series of layers that progressively downsample to a bottleneck layer, at which point the process is reversed. Such a network requires that all information pass through all the layers. Therefore, there is a great deal of low-level information shared in the input and output, and is desirable to shuttle this information across the net directly. In order to circumvent the bottleneck for information like this, U-net structure [12] is employed to give the generator. The U-Net based generator module network is diagrammed in Figure 3. The input of the U-Net based generator module is a noisy and blurring image containing "real" faint dot matrix information, and the output is the generated faint dot matrix image. The U-Net based generator consists of the downsampling part, the innermost layer part and the upsampling part. The downsampling part includes 5 convolution+ReLU layers and 4 Maxpooling layers. The innermost layer part contains the convolution+ReLU and the deconvolution+ReLU. The upsampling part includes 3 deconvolution+ReLU layers, 2 unpooling layers and deconvolution+Tanh layer that is also the output layer. The convolution kernel size is 4×4, the stride is 2, and the padding is 1.

3.1.2 The PatchGAN Discriminator. In order to model the high-frequency faint invisible dot matrix image structure, the attention is turned to the structure in the local image patches. Thus, the PatchGAN discriminator architecture module is given as shown in Figure 4 to penalize the structure at the scale of patches. This discriminator can classify when the $m \times m$ patch in the image is real or fake. The ultimate output of the discriminator is obtained via running the discriminator convolutionally across the whole image and averaging all responses. In proposed PatchGAN discriminator architecture, the size of the patch is 256×256. The first layer is the convolution+Leaky ReLu with 64 filters. The second layer, third layer and fourth layer are the convolution+BatchNorm+Leaky ReLu with 128, 256 and 512 filters, respectively. After the last layer, a convolution is applied to map to a 1-dimensional output, followed by a sigmoid function.

3.2 Loss Function

Similar to other GANs, the core of proposed U-Net GAN is also derived from the zero-sum game in the game theory [40]. The generator loss is

$$\mathcal{L}_G = \mathbb{E}_I(\log(1 - D(G(I)))), \tag{4}$$

And the objective corresponding to the discriminator is

$$-\mathcal{L}_D = \mathbb{E}_J(D(J)) + \mathbb{E}_I(\log(1 - D(G(I)))), \tag{5}$$

The objective of GAN is denoted as

$$\mathcal{L}_{GAN} = \mathcal{L}_G - \mathcal{L}_D. \tag{6}$$

In order to encourage less blurring for the dot matrix image, L_1 loss is used as

$$\mathcal{L}_{L_1} = \mathbb{E}_{I,J}(\|J - G(I)\|_1). \tag{7}$$

For the sake of convenience, let $\tilde{J} = G(I)$. a roughening term is introduced in the loss function to further enhance the model's focus on high-gradient and low-contrast areas. The roughening term can help the model pay more attention to specific areas of the image that are critical for anti-counterfeiting features. The roughening

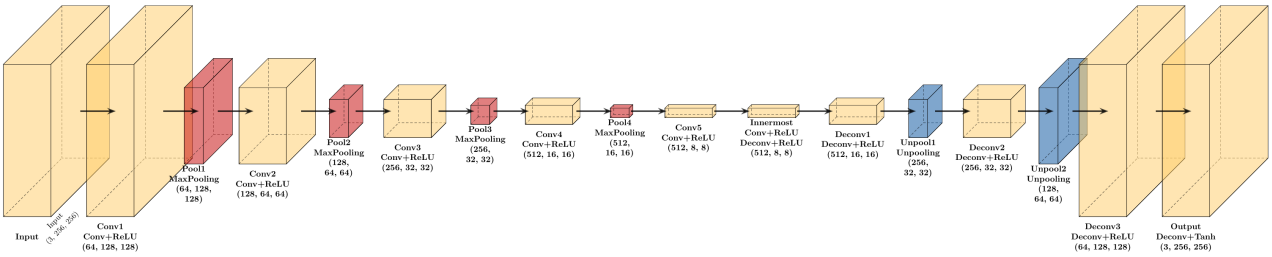

Fig. 3: The U-Net based generator module network.

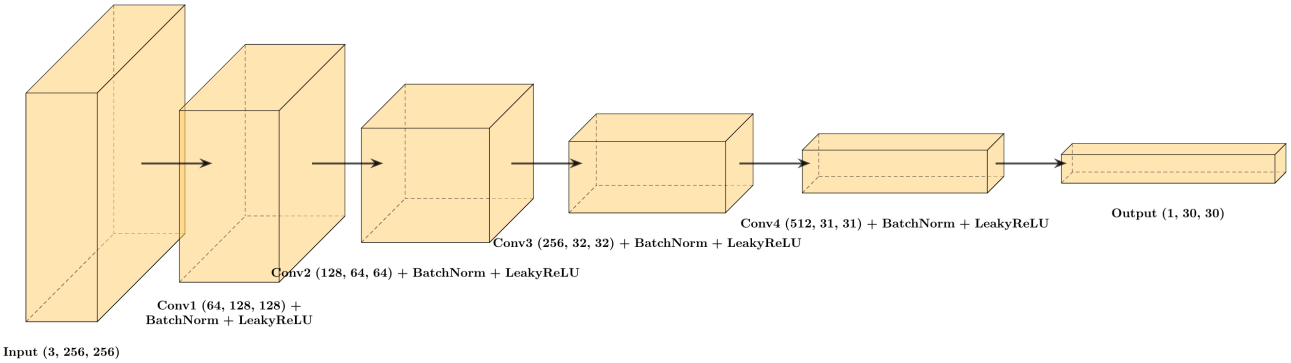

Fig. 4: The discriminator architecture module.

loss function is achieved by focusing on the second-order spatial derivatives (Laplacian) of the images:

$$\mathcal{L}_{\text{rough}} = \sum_{x,y} \left(\nabla^2 J(x,y) - \nabla^2 \tilde{J}(x,y) \right)^2, \tag{8}$$

where ∇^2 denotes the Laplacian operator, which is defined as:

$$\nabla^2 J(x,y) = \frac{\partial^2 J}{\partial x^2} + \frac{\partial^2 J}{\partial y^2}. \tag{9}$$

The roughening term encourages the preservation and enhancement of fine details by penalizing discrepancies in the higher-order derivatives between the true and fake images.

To enhance the model's sensitivity to high-gradient changes, the Gradient-Sensitive Activation (GSA) function is introduced in this study. The GSA function is designed to emphasize areas with significant gradient changes, preserving more details during the image restoration process. The GSA function can be defined as follows:

$$GSA(x) = \begin{cases} x^2 & \text{if } x < 0 \\ \sqrt{x} & \text{if } x \geq 0. \end{cases} \tag{10}$$

This function allows the model to respond more effectively to high-gradient areas, ensuring that fine details in the dot matrix patterns are accurately captured and restored.

The GSA function based loss term $\mathcal{L}_{\text{GSA}}$ focuses on high-gradient areas to improve the detection of fine structures. The loss term $\mathcal{L}_{\text{GSA}}$ is defined as:

$$\mathcal{L}_{\text{GSA}} = \sum_{x,y} \left(GSA(\nabla J(x,y)) - GSA(\nabla \tilde{J}(x,y)) \right)^2, \tag{11}$$

where ∇J and $\nabla \tilde{J}$ represents the gradient of the image J and $\tilde{J} = G(I)$, respectively. The gradient of the image ∇J is computed as:

$$\nabla J(x,y) = \left(\frac{\partial J}{\partial x}, \frac{\partial J}{\partial y} \right). \tag{12}$$

This term emphasizes regions with significant gradient changes, ensuring that the restored image accurately captures fine structures and details.

Therefore, our final objective is

$$G^* = \arg\min_G \max_D \mathcal{L}_{GAN} + \lambda_{L_1} \mathcal{L}_{L_1} + \lambda_{\text{rough}} \mathcal{L}_{\text{rough}} + \lambda_{\text{GSA}} \mathcal{L}_{\text{GSA}}, \tag{13}$$

where λ_{L_1}, λ_{rough}, and λ_{GSA} are the super-parameters controlling the trade-off among all the loss terms. The generator G and discriminator D enhance each other in the confrontation and arrive at an equilibrium state eventually.

3.3 Dynamic Weight Adjustment Mechanism

To optimize the image restoration process, a dynamic weight adjustment mechanism is implemented based on decoding rate feedback. This mechanism adjusts the network weights dynamically, ensuring that the model adapts to the varying complexities of the input images. The dynamic weight adjustment formula is given by:

$$w_{\text{new}} = w_{\text{old}} + \eta \cdot \frac{\partial \mathcal{L}}{\partial w} \cdot D_{\text{rate}}, \tag{14}$$

where η is the learning rate, and D_{rate} represents the decoding rate, reflecting feedback on the model's current decoding performance. This adaptive approach ensures that the model continuously im-

proves its restoration and decoding capabilities, leading to higher accuracy and reliability.

4. EXPERIMENTS

To validate the effectiveness of our proposed approach, extensive experiments are conducted using a dataset of printed faint dot matrix images. The detailed courses include the following steps:

4.1 Experimental Settings

The hardware configure of the experimental platform is E5-2683 V3 processor and Nvidia Titan Xp graphics card. The operating system for platform run is Ubuntu 20.04 operating system, and the framework for deep learning is Pytorch 1.8.1. The loss functions for both U-Net based generator and PatchGAN discriminator are optimized by the Adam optimizer [41], with a learning rate of 0.0002, and momentum parameters $\beta_1 = 0.5$, $\beta_2 = 0.999$. In the experiment, the super-parameters in the objective are set to $\lambda_{L_1} = 100$, $\lambda_{\text{rough}} = \lambda_{\text{GSA}} = 150$. The generator network and discriminator network is trained alternatively with the batch size equal to 1, and the number of iterative training epochs is 100.

4.2 Dataset

Because there is currently no data set related to printed faint dot matrix images, a dataset of dot matrix images is created with different car logos, which are composed of "real" faint dot matrix for anti-counterfeiting and different trademark images with some noisy and blurring information. The dataset contains 3,000 images with a resolution of 256×256 pixels. It is divided into three parts that are 2000 samples used as the training set, 350 samples used as the validation set, and 650 samples used as the test set. Each sample has the real faint dot matrix image corresponding to the real image J in the section 3. For example, Figure 5 shows one of the pairs composed of real faint dot matrix images and dot matrix images with different noisy and blurring car logo backgrounds. The real faint dot matrix image is shown in Figure 5 (a), and the noisy and blurring image containing the corresponding real faint dot matrix information is shown in Figure (b). This dataset can not only satisfy the research in this paper, but also provide the convenience of other research on the feature extraction of printed quantum dots, and reduce the time spent on image preprocessing and formatting in the future.

4.3 Evaluation Metrics

For the quantitative evaluation metrics such as Peak Signal-to-Noise Ratio (PSNR), Structural Similarity Index (SSIM) given in [42] are used to evaluate the performance of our approach. In additional, the evaluation metrics for dot matrix images are designed to quantify the similarity between two dot matrix images. These images typically contain numerous discrete points, and their distribution and density are crucial for image quality and feature recognition. Similarity calculation compares the pixel values at the same positions in dot matrix images. First, define the total number of pixels:

$$\text{total\_pixels} = m \times n, \tag{15}$$

where m and n are the number of rows and columns of the dot matrix image, respectively. Then, calculate the number of matching

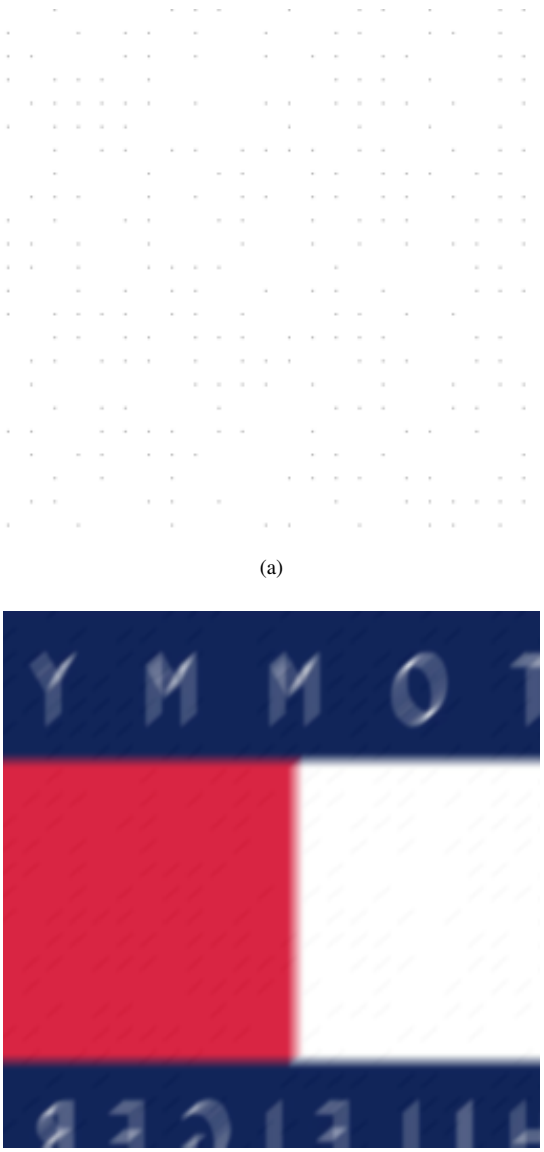

(a)

(b)

Fig. 5: (a)Real Faint Dot Matrix Image, (b)Noisy and Blurring Image Containing the Corresponding Real Faint Dot Matrix Information

pixels by

$$\text{matching\_pixels} = \sum_{i=0}^{m-1} \sum_{j=0}^{n-1} (\text{matrix1}[i][j] == \text{matrix2}[i][j]). \tag{16}$$

Finally, the Similarity Percentage (SP) is given as the following

$$\text{SP} = \left(\frac{\text{matching\_bits}}{\text{total\_bits}} \right) \times 100\%. \tag{17}$$

4.4 Experimental Results

In order to verify the effectiveness of proposed method for image clarity, readability, and decoding accuracy for the faint dot matrix

images, the model training effect is checked on the validation set and the learning ability is tested on the test set. Firstly, randomly choose 8 noisy and blurring images containing "real" faint dot matrix information from the test set. Then use our trained model to test these images to recover the faint dot matrix images. The first four noisy and blurring images containing "real" faint dot matrix information and the corresponding recovery results are shown in Figure 6. The last four noisy and blurring images containing "real" faint dot matrix information and the corresponding recovery results are shown in Figure 7.

By observing these experimental results, we can see that the quality of recovery faint dot matrix images is very good. Table 1 shows PSNR, SSIM and the Similarity Percentage (SP) values for the 8 recovery faint dot matrix images.

The experimental results demonstrate that our method significantly has the dot matrix image clarity, readability, and decoding accuracy. In summary, our innovative approach integrating U-Net with GANs, enhanced by the GSA function, Roughening term, decoding module with feedback mechanism, and dynamic weight adjustment mechanism, provides a robust solution for the restoration and decoding of printed faint dot matrix images. This methodology not only improves anti-counterfeiting technologies but also sets a new standard for high-gradient image enhancement and security feature detection.

5. DISCUSSION

In order to enhance the efficiency of the restoration for the faint dot matrix images, and reduce the time spent on our deep learning model in the future research, we give the preprocessing method for RGB dot matrix images dataset used above in the section 4.2. This preprocessing pipeline includes the following stages:

5.1 Preprocessing of Dot Matrix Images

The initial step involves preprocessing the dot matrix images to standardize the input data and enhance the efficiency of subsequent processing steps. This preprocessing pipeline includes the following stages:

5.1.1 Grayscaling. The input images are converted to grayscale to reduce computational complexity and focus on the essential features for restoration. The grayscale conversion formula is:

$$I_{\text{gray}} = 0.299 \cdot I_R + 0.587 \cdot I_G + 0.114 \cdot I_B, \tag{18}$$

where I_R, I_G, and I_B are the red, green, and blue channels of the image, respectively.

5.1.2 Binarization. A thresholding technique is applied to binarize the grayscale images, converting them into binary images that highlight the dot matrix patterns against the background. The Otsu method is used for thresholding, with the formula:

$$\sigma_B^2 = \omega_1(\mu_1 - \mu_T)^2 + \omega_2(\mu_2 - \mu_T)^2, \tag{19}$$

where ω_1 and ω_2 are the weights of the two classes, μ_1 and μ_2 are the means of the two classes, and μ_T is the global mean. The threshold that maximizes the inter-class variance σ_B^2 is selected.

5.1.3 Noise Filtering. Various noise reduction techniques, such as Gaussian blurring and median filtering, are applied to remove background noise and enhance the visibility of the dot matrix patterns. The formula for Gaussian blurring is:

$$I_{\text{blur}}(x, y) = \frac{1}{2\pi\sigma^2} \exp\left(-\frac{x^2 + y^2}{2\sigma^2}\right) * I(x, y), \tag{20}$$

where σ is the standard deviation of the Gaussian function, and $*$ denotes the convolution operation.
These preprocessing steps ensure that the input data fed into the deep learning models is clean and standardized, facilitating more accurate restoration and decoding of the faint dot matrix images.

6. CONCLUSION

In this paper, we propose an innovative image processing approach that integrates U-Net with Generative Adversarial Networks (GANs) for recovering the faint dot matrix images, aiming to enhance the application of anti-counterfeiting technologies. We employ U-Net based architecture as the generator and use a convolutional PatchGAN classifier as the discriminator to form our U-Net based GAN model. This method accurately extracts faint anti-counterfeiting features within complex noisy and blurring backgrounds, significantly improving image clarity and readability. We introduce an activation function called Gradient-Sensitive Activation (GSA), which enhances the model's sensitivity to high-gradient changes in the image, thereby preserving more detail information during faint dot matrix image restoration. In order to further improve model performance and adaptability, we incorporate a roughening term in the loss function make the model to focus more on the high-gradient or low-contrast areas to effectively enhance the recognition and restoration capabilities for subtle anti-counterfeiting features. Moreover, the system dynamically adjusts network weights based on decoding rate feedback to optimize the image restoration process. Experimental results demonstrate that this method has image clarity, readability, and decoding accuracy for the recovery faint dot matrix images.

Additionally, In order to enhance the efficiency of the recovering for the faint dot matrix images, and reduce the time spent on our deep learning model in the future research, we give the preprocessing method for RGB dot matrix images dataset according to the grayscaling stage, binarization stage and noise filtering stage. And to further strengthen the this study, a more extensive evaluation considering various datasets or scenarios will be collected to enhance the research in the future.

This paper not only demonstrates the potential application of deep learning in image anti-counterfeiting technology but also provides a new perspective and methodology for the future research in image processing technology. Our method is expected to play an increasingly significant role in protecting intellectual property, ensuring data security, and combating illegal reproductions.

7. REFERENCES

[1] Teymournezhad, K.; Azgomi, H.; Asghari, A. Detection of counterfeit banknotes by security components based on image processing and GoogLeNet deep learning network. *Signal, Image and Video Processing* **2022**, *16*, 1505–1513.

[2] Liang, T.; et al. Design and Recognition of Cigarette Anti-counterfeiting Code Based on OpenCV. In Proceedings of the *2023 IEEE 5th International Conference on Civil Aviation Safety and Information Technology (ICCASIT)*, 2023; pp. 307–312.

[3] Zheng, Z.; et al. Circumferential Local Ternary Pattern: New and Efficient Feature Descriptors for Anti-Counterfeiting Pattern Identification. *IEEE Transactions on Information Forensics and Security* **2022**, *17*, 970–981.

[4] Ren, M.; Xu, J. An improved CLAHE image enhancement algorithm for dot matrix invisible code. In Proceedings of the

Table 1. PSNR, SSIM, and SP values for the 8 recovery faint invisible dot matrix images.

Recovery Faint Dot Matrix Image No.	PSNR	SSIM	SP
1	47.9502 dB	0.9814	96.60%
2	48.3772 dB	0.9804	97.16%
3	48.6779 dB	0.9839	97.46%
4	47.2048 dB	0.9725	96.21%
5	47.5901 dB	0.9731	96.38%
6	48.6674 dB	0.9884	97.43%
7	49.0044 dB	0.9891	97.49%
8	47.8132 dB	0.9754	96.46%

International Conference on Electronic Technology and Information Science, 2023.

[5] Zhang, W.; et al. Research progress of applying digital watermarking technology for printing. In Proceedings of the *2018 Chinese Control And Decision Conference (CCDC)*, 2018; pp. 4479–4482.

[6] Rossi, R.; et al. Novel computer generated holograms for high-security anti-counterfeiting applications. 2017.

[7] Gao, Y. On the Use of Overt Anti-Counterfeiting Technologies. *Mark. Sci.* **2018**, *37*, 403–424.

[8] Goodfellow, I.J.; et al. Generative adversarial networks. *Communications of the ACM* **2014**, *63*, 139–144.

[9] Kingma, D.P.; Welling, M. Auto-Encoding Variational Bayes. *CoRR* **2013**, abs/1312.6114.

[10] Hendry; Manongga, D.H.F.; Nataliani, Y.; Wellem, T. Anti-Counterfeit Handwritten Signature via DCGAN with SGPD Network. In Proceedings of the *2021 7th International Conference on Applied System Innovation (ICASI)*, Chiayi, Taiwan, 2021; pp. 79–84.

[11] Lee, S. H.; Lee, H. Y. Counterfeit Bill Detection Algorithm using Deep Learning. *International Journal of Applied Engineering Research* **2018**, *13*, 304–310.

[12] Ronneberger, O.; et al. U-Net: Convolutional Networks for Biomedical Image Segmentation. *ArXiv* **2015**, abs/1505.04597.

[13] Wu, H.; Kong, X.; Shang, S. A Printer Forensics Method using Halftone Dot Arrangement Model. In Proceedings of the *2015 IEEE China Summit and International Conference on Signal and Information Processing*, Chengdu, China, 2015; pp. 861–865.

[14] Liu, Y.; et al. Dot-Diffused Halftoning with Improved Homogeneity. *IEEE Transactions on Image Processing* **2015**, *24*, 4581–4591.

[15] Liu, Y.; et al. New Class Tiling Design for Dot-Diffused Halftoning. *IEEE Transactions on Image Processing* **2013**, *22*, 1199–1208.

[16] Son, C. Estimating Embedded Data from Clustered Halftone Dots via Learned Dictionary. In Proceedings of the *2014 IEEE International Conference on Image Processing (ICIP)*, Paris, France, 2014; pp. 2624–2628.

[17] Yuan, B.; et al. Research on Enhancement and Extraction Algorithms of Printed Quantum Dots Image Using A Generative Adversarial Network. *International Journal of Science and Technology Research* **2021**, *10*, 116–124.

[18] Qiu, Y.; et al. Information Recognition of Printed Quantum Dots Matrix Image under Uncorrected Conditions. In Proceedings of the *2022 4th International Conference on Robotics and Computer Vision (ICRCV)*, Wuhan, China, 2022; pp. 37–42.

[19] Chen, G.; et al. Quantum Dots-Based All-Optical-Readout Middle-Far-Infrared Imaging. *IEEE Journal of Quantom Electronics* **2011**, *47*, 285–292.

[20] Hu, S.; et al. An Ethanol Vapor Sensor Based on A Microfiber with A Quantum-Dot Gel Coating. *Sensors* **2019**, *19300*, 1–7.

[21] Esfahani, A. M.; et al. Developing A Superlens with High Resolution Using Quantum Dot Nano-Particles. In Proceedings of the *2023 31st International Conference on Electrical Engineering (ICEE)*, Tehran, Iran, 2023; pp. 600–604.

[22] Li, Q.; et al. The Method of Error Controlling on the Vectorization of Dot Matrix Image. In Proceedings of the *2008 International Conference on Computer Science and Software Engineering*, Wuhan, China, 2008; pp. 810–813.

[23] Xu, G.; et al. Optimize Geometry Division to Construct Clustered Dot Dithering Matrix. In Proceedings of the *2010 Second International Conference on Computer Modeling and Simulation*, Sanya, China, 2010; pp. 414–417.

[24] Cheng, Y.; et al. A Scanning Method for Dotted Data Matrix. In Proceedings of the *2008 Eighth International Conference on Intelligent Systems Design and Applications*, Kaohsiung, Taiwan, 2008; pp. 179–183.

[25] Patki, S. N.; et al. Dot Matrix Text Recognition for Industrial Carton Classification. In Proceedings of the *2015 International Conference on Intrustrial Instrumentation and Control (ICIC)*, Pune, India, 2015; pp. 777–782.

[26] Xu, X.; et al. Image Recognition Technique for Dot-matrix Character on Piston Surface Based on Hopfield Neural Network Method. In Proceedings of the *2010 International Conference on Audio, Language and Image Processing*, Shanghai, China, 2010; pp. 320–323.

[27] Ge, J.; et al. Recognition of Dot-Matrix Character-Degraded Based on Affine Registration. In Proceedings of the *2019 14th IEEE International Conference on Electronic Measurement and Instruments (ICEMI)*, Changsha, China, 2019; pp. 405–412.

[28] Chen, R.; et al. Customized 2D Barcode Sensing for Anti-Counterfeiting Application in Smart IoT with Fast Encoding and Information Hiding. *Sensors* **2020**, *23795*, 1–19.

[29] Wang, T.; et al. A Texture-Hidden Anti-Counterfeiting QR Code and Authentication Method. *Sensors* **2023**, *23795*, 1–25.

[30] Wu, W. R.; et al. Image Restoration Using Fast Modified Reduced Update Kalman Filter. *IEEE Transactions on Signal Processing* **1992**, *40*, 915–926.

[31] Citrin, S.; et al. A Full-Plane Block Kalman Filter for Image Restoration. *IEEE Transactions on Image Processing* **1992**, *22*, 473–487.

[32] Lung, H.; et al. Noise Adaptive Soft-Switching Median Filter. *IEEE Transactions on Image Processing* **2001**, *10*, 242–251.

[33] Dong, Y.; et al. Image Restoration Technique for 3D Laser Scanning Images. In Proceedings of the *2022 IEEE 9th International Conference on Electronics, Circuits and Systems (ICECS)*, Nicosia, Cyprus, 2022; pp. 273–277.

[34] Qi, X.; et al. A New Image Restoration Approach for Low-Light and Noisy Images Using Deep Learning and Enhancement Methods. In Proceedings of the *2023 International Conference on Image Processing and Pattern Recognition (IPPR)*, Shanghai, China, 2023; pp. 19–24.

[35] Li, L.; et al. Multi-Scale Convolutional Neural Network for Image Restoration Based on Wavelet Transform. *IEEE Access* **2019**, *7*, 24564–24573.

[36] Li, C.; et al. Precomputed Real-Time Texture Synthesis with Markovian Generative Adversarial Networks. In Proceedings of the *ECCV 2016,* , Part III, LNCS 9907, 2016; pp. 702–716.

[37] Schonfeld, E.; et al. A U-Net Based Discriminator for Generative Adversarial Networks. In Proceedings of the *IEEE/CVF International Conference on Computer Vision*, Montreal, QC, Canada, 2021; pp. 10–17.

[38] Cheng, S.; et al. SUGAN: A Stable U-Net Based Generative Adversarial Network. *Sensors* **2023**, *237338*, 1–20.

[39] Hinton, G. E.; et al. Reducing the Dimensionality of Data with Neural Networks. *Science* **2006**, *313*, 504–507.

[40] Sun, K.; et al. Deep high-resolution representation learning for human pose estimation. In Proceedings of the *IEEE/CVF International Conference on Computer Vision*, Long Beach, CA, USA, 2019; pp. 15–20.

[41] Kingma, D.; et al. Adam: A Method for Stochastic Optimization. In Proceedings of the *International Conference on Learning Representation*, San Diego, CA, USA, 2015; pp. 1–15.

[42] Wang, Z.; et al. Image Quality Assessment: From Error Visibility to Structural Similarity. *IEEE Transactions on Image Processing* **2004**, *13*, 600–612.

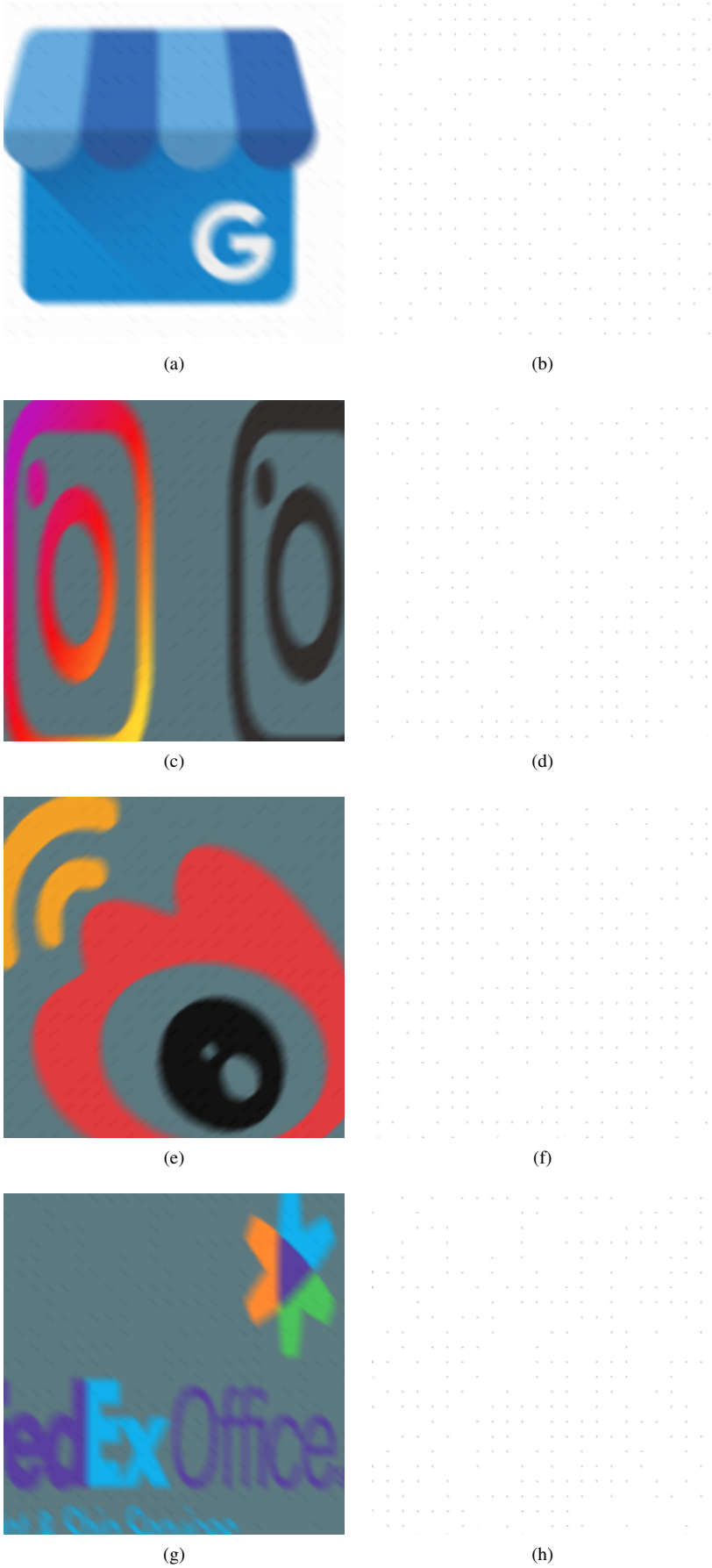

(a) (b)

(c) (d)

(e) (f)

(g) (h)

Fig. 6: (a),(c),(e) and (g) are noisy and blurring images, and (b),(d),(f) and (h) are corresponding recovery results.

(a)

(b)

(c)

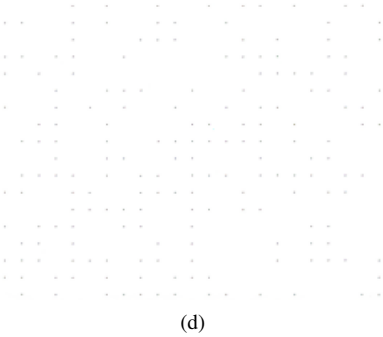

(d)

(e)

(f)

(g)

(h)

Fig. 7: (a),(c),(e) and (g) are noisy and blurring images, and (b),(d),(f) and (h) are corresponding recovery results.